Rapid Phosphotransfer to CheY from a CheA Protein Lacking the CheY-Binding Domain†

Richard C. Stewart,*,‡ Knut Jahreis,§,|| and John S. Parkinson§

Department of Cell Biology and Molecular Genetics, University of Maryland, College Park, Maryland 20742, and Department of Biology, University of Utah, Salt Lake City, Utah 84112

Received May 15, 2000; Revised Manuscript Received August 14, 2000

ABSTRACT: The histidine protein kinase CheA plays a central role in the bacterial chemotaxis signal transduction pathway. Autophosphorylated CheA passes its phosphoryl group to CheY very rapidly ($k_{cat} \sim 750\ s^{-1}$). Phospho-CheY in turn influences the direction of flagellar rotation. The autophosphorylation site of CheA (His^{48}) resides in its N-terminal P1 domain. The adjacent P2 domain provides a high-affinity binding site for CheY, which might facilitate the phosphotransfer reaction by tethering CheY in close proximity to the phosphodonor located in P1. To explore the contribution of P2 to the CheA → CheY phosphotransfer reaction in the *Escherichia coli* chemotaxis system, we examined the transfer kinetics of a mutant CheA protein (CheAΔP2) in which the 98 amino acid P2 domain had been replaced with an 11 amino acid linker. We used rapid-quench and stopped-flow fluorescence experiments to monitor phosphotransfer to CheY from phosphorylated wild-type CheA and from phosphorylated CheAΔP2. The CheAΔP2 reaction rates were significantly slower and the K_m value was markedly higher than the corresponding values for wild-type CheA. These results indicate that binding of CheY to the P2 domain of CheA indeed contributes to the rapid kinetics of phosphotransfer. Although phosphotransfer was slower with CheAΔP2 ($k_{cat}/K_m \sim 1.5 \times 10^6\ M^{-1}\ s^{-1}$) than with wild-type CheA ($k_{cat}/K_m \sim 10^8\ M^{-1}\ s^{-1}$), it was still orders of magnitude faster than the kinetics of CheY phosphorylation by phosphoimidazole and other small molecule phosphodonors ($k_{cat}/K_m \sim 5-50\ M^{-1}\ s^{-1}$). We conclude that the P1 domain of CheA also makes significant contributions to phosphotransfer rates in chemotactic signaling.

The chemotaxis signaling system of *Escherichia coli* enables cells to make rapid adjustments of their swimming patterns in response to chemical gradients in their environment (*1*). Cell surface chemoreceptors monitor attractant and repellent levels and communicate stimulus information to the flagellar rotary motors through two intracellular proteins, CheA and CheY (*2*). CheA is a histidine protein kinase (HPK)[1] (*3*, *4*) whose activity is modulated by the chemoreceptors (*5*−*8*). CheA activity in turn controls the phosphorylation state of CheY, a response regulator (RR). Phospho-CheY (P-CheY) controls the cell's swimming behavior by interacting directly with flagellar motors to enhance their probability of clockwise (CW) rotation (*9*, *10*).

The CheA → CheY signaling transaction is one of the most intensively studied examples of a His−Asp phosphorelay (*11*), the hallmark of "two-component" signal transduction pathways in a wide variety of microorganisms and higher plants (*12*, *13*). CheA first autophosphorylates at a histidine residue (His^{48}) utilizing the γ-phosphoryl group of ATP (*3*). The phosphoryl group from P-CheA is then transferred to an aspartate residue (Asp^{57}) in CheY (*14*). The CheA → CheY phosphotransfer reaction is most likely catalyzed by CheY, which can also autophosphorylate, albeit much less rapidly, using small molecule phosphodonors such as acetyl phosphate (*15*) and phosphoimidazole (*16*). Crystal structures and NMR-derived structures have been reported for CheA (*17*, *18*) and CheY (*19*, *20*) and a CheA·CheY complex (*21*, *22*). This structural information and extensive mutagenesis studies have made CheA and CheY two of the best characterized members of the HPK and RR superfamilies, respectively, and excellent experimental models for exploring mechanistic features of two-component signaling pathways.

One feature of the chemotaxis system that distinguishes it from most other two-component systems is the impressive speed at which it operates. Most two-component signaling systems regulate gene expression and operate on a time scale of minutes. By contrast, *E. coli* needs only 50−100 ms to detect and respond to chemotactic stimuli (*23*, *24*). This means that the underlying phosphorylation events must operate on a subsecond time scale to generate appropriate changes in P-CheY levels. In previous work, we demonstrated that phosphotransfer from P-CheA to CheY takes place on a millisecond time scale ($k_{cat} \sim 750\ s^{-1}$) (*25*, *26*). His−Asp phosphotransfers are much less rapid in two-

† This research was supported by Research Grants GM52583 (to R.C.S.) and GM19559 (to J.S.P.) from the National Institutes of Health.

* Corresponding author. Phone: (301) 405-5475. Fax: (301) 314-9489. E-mail: rs224@umail.umd.edu.

‡ University of Maryland.

§ University of Utah.

|| Present address: Fachbereich Biologie/Chemie, Universität Osnabrück, 49069 Osnabrück, Germany.

[1] Abbreviations: CCW, counterclockwise; CW, clockwise; P-CheA, phosphorylated CheA; P-CheY, phosphorylated CheY; HPK, histidine protein kinase; RR, response regulator.

10.1021/bi001100k CCC: $19.00
Published on Web 10/04/2000

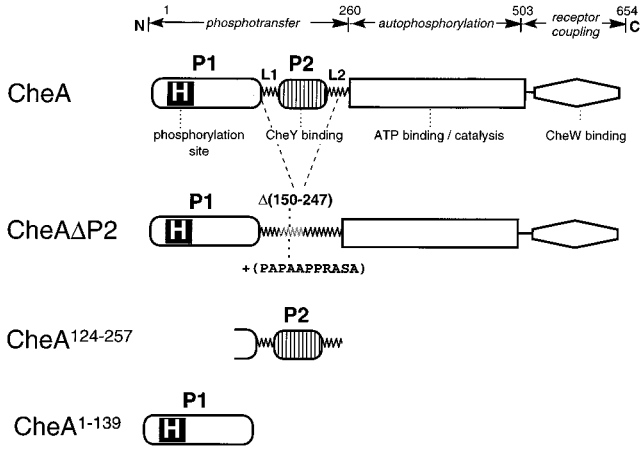

FIGURE 1: Functional organization and important structural features of wild-type CheA, CheAΔP2, CheA$^{124-257}$, and CheA$^{1-139}$. The indicated regions have been defined as discrete structural and functional domains (*17*, *29*). In CheAΔP2, amino acids 150−247 were replaced by an 11-residue sequence as indicated. CheA$^{124-257}$ encompasses all of P2 plus flanking sequences at its N- and C-termini. CheA$^{1-139}$ encompasses all of P1.

component signaling systems that regulate gene expression rather than locomotion. For example, phosphotransfer from VanS to its cognate response regulator, VanR (a transcriptional regulator), operates on a considerably slower time scale ($k_{cat} \sim 1.6\ s^{-1}$) (*27*). Detailed kinetic analyses have not been reported for other two-component systems, but qualitative results from these systems support the general conclusion that phosphotransfer reactions in the chemotaxis system are at least 100−1000-fold faster than the corresponding reactions in the nonchemotaxis two-component systems (*13*, *27*, *28*). What features of CheA and CheY account for the very fast phosphotransfer rate relative to other two-component systems? Understanding how these features contribute to the rate of CheA → CheY phosphotransfer should provide important insight into how the basic chemistry of His−Asp phosphorelays can be fine-tuned to meet specific signaling needs.

The unique architecture of the CheA protein may be responsible for its rapid phosphotransfer ability (*17*, *29*−*31*). The N-terminal third of CheA contains two domains (P1 and P2) that play key roles in phosphotransfer to CheY (Figure 1). The P1 domain contains the autophosphorylation site (*3*, *29*) and must, therefore, interact with CheY during phosphotransfer. The adjacent P2 domain contains a binding site for CheY (*29*, *32*), which presumably facilitates phosphotransfer by placing CheY in close proximity to the phosphorylated histidine side chain in P1. CheY docking at P2 might also contribute to catalysis of phosphotransfer by several other mechanisms, such as (i) promoting productive orientation of Asp^{57} in CheY and phospho-His^{48} in CheA, (ii) inducing a CheY conformation that enhances its reactivity, and (iii) providing catalytic groups that promote steps in phosphotransfer. To assess the contributions of P2 to the CheA → CheY phosphotransfer reaction, we constructed a CheA variant (CheAΔP2) lacking the P2 domain but still capable of autophosphorylation and phosphotransfer. Here we show that phosphotransfer to CheY from CheAΔP2 is ∼25-fold slower than from wild-type CheA but still many orders of magnitude faster than from a small molecule phosphodonor. These findings indicate that both the P1 domain and the P2 domain make important contributions to the phosphotransfer reaction.

EXPERIMENTAL PROCEDURES

Protein Preparations. CheY and CheA were purified following published methods (*4*, *33*). Wild-type CheA was purified from cells [*E. coli* strain RP3098 (*34*)] carrying plasmid pKJ9 (*35*). The same procedure was used to isolate CheAΔP2 from cells carrying plasmid pKJ9-1.1. These expression plasmids carried the appropriate *cheA* coding region preceded by four in-frame codons of the parental plasmid pTM30 (*36*). The additional N-terminal residues have no discernible effect on the in vitro or in vivo activity of CheA (*35*). Plasmid pKJ9-1.1 was created by deleting (from plasmid pKJ9) the portion of *cheA* encoding amino acids 150−247. To accomplish this, oligonucleotide-directed mutagenesis was used to create a *Sac*II restriction site in the L1 linker of the *cheA* coding sequence in pKJ9. Then, a double-stranded oligonucleotide, encoding an alanine/proline-rich linker, was inserted between the introduced *Sac*II site and an *Eag*I site in the L2 linker segment to create the ΔP2 construct. This construct was confirmed by sequencing the entire *cheA* gene in the mutant plasmid. CheY and CheA protein concentrations were determined spectrophotometrically using extinction coefficients (8.25 $mM^{-1}\ cm^{-1}$ for CheY; 16.3 $mM^{-1}\ cm^{-1}$ for CheA) calculated by the method of Gill and von Hippel (*37*).

CheA fragments corresponding to various functional domains of the full-length protein were purified by making use of plasmids that directed overexpression of the corresponding segments of the *cheA* coding sequences. CheA$^{124-257}$ (a fragment of CheA encompassing the P2 domain) was purified from cells (RP3098) carrying plasmid pTM22 as reported previously (*38*). CheA$^{1-139}$ (corresponding to the P1 domain) was overproduced using a derivative of plasmid pET14 (Novagen) that fused an N-terminal $(His)_6$ affinity tag to the protein, allowing purification of the $(His)_6$-CheA$^{1-139}$ fusion by the procedure of Levit et al. (*39*). The concentrations of CheA$^{124-257}$ and $(His)_6$-CheA$^{1-139}$ were determined using the BCA assay kit from Pierce Chemical Co. with bovine serum albumin serving as the standard.

The phosphorylated form of wild-type CheA was generated as described previously (*4*). Phosphorylated $(His)_6$-CheA$^{1-139}$ was generated via transphosphorylation (*39*) by incubating 50 μM $(His)_6$-CheA$^{1-139}$ with 5 μM CheA$^{98-654}$ [purified as described previously (*33*)] in the presence of 5 mM ATP and 10 mM $MgCl_2$. The phosphorylated $(His)_6$-CheA$^{1-139}$ was then isolated from the reaction mixture by Ni^{2+}−NTA chromatography (thereby removing the CheA$^{98-654}$ and ATP).

Experiments To Monitor Phosphotransfer Time Courses. All phosphotransfer experiments were carried out in TMD buffer (50 mM Tris, 10 mM $MgCl_2$, 0.5 mM DTT, pH 7.5). Quench-flow experiments were performed using a BioLogic QFM-5 instrument as described previously (*25*). For most such experiments, 60 μL of ^{32}P-CheAΔP2 (0.1−0.5 μM before mixing) was mixed with 60 μL of CheY (1−60 μM before mixing). The resulting mixture passed through an aging line for a predetermined time interval before being mixed with an equal volume of quench buffer (10% SDS, 0.1 M EDTA, 50 mM Tris-HCl, pH 6.8). Samples were then

analyzed by SDS−PAGE (on 17% gels) followed by phosphoimager analysis to quantify the level of ^{32}P associated with P-CheAΔP2 and P-CheY at each time point. Each reaction was performed in at least two independent experiments in which duplicate samples were averaged for each time point.

Stopped-flow fluorescence experiments were performed and analyzed using an Applied Photophysics SX.17MV instrument as described previously (*26*). In a typical experiment, 50 μL of P-CheAΔP2 was mixed with an equal volume of CheY solution, and the ensuing changes in CheY intrinsic fluorescence were monitored. Time courses from 10 to 15 consecutive "shots" were averaged to improve the signal-to-noise ratio.

Computer Simulations of the Effect of Decreasing k_{phos}, the Rate Constant Controlling Phosphotransfer Kinetics. To explore how the overall efficacy of the chemotaxis system would be affected by altering the rate of the CheA phosphotransfer to CheY and CheB,[2] we used BCT version 4.2 developed by Bourret, Lay, Levin, and Bray (*40*, *41*) (downloaded from URL http://www.zoo.cam.ac.uk/zoostaff/levin/Chemotaxis.html). This program represents the chemotaxis signaling system as a set of differential equations and makes use of experimentally determined rate constants, defined binding association constants, and known intracellular concentrations of the Che proteins. On the basis of this information, the program uses numerical integration to calculate the resulting concentration of P-CheY (and other signaling intermediates). In addition, BCT can simulate the effect of exposing the system to a chemotaxis stimulus (attractant or repellent). We made use of this feature to examine the response of the system to a 3 μM down-jump in aspartate concentration. Aspartate is an effective chemoattractant that binds to the receptor Tar with a K_d of ~3 μM (*42*); thus our "test stimulus" served to activate half of the cell's pool of Tar, and this is reflected in a corresponding increase in the kinase activity of CheA associated with these Tar molecules which, in turn, generates a transient increase in the P-CheY level (*5*, *6*). These computer simulations calculated the concentration of P-CheY (Figure 6A) in unstimulated cells (prior to addition of aspartate) and in stimulated cells (maximal P-CheY value generated within 1 s after removal of the aspartate).

BCT represents each protein−protein interaction as a simple second-order reaction (e.g., rate of phosphotransfer $= k_{phos}$[CheY][P-CheA]). The rate constants used for these interactions are based on experimental measurements and are provided as part of the BCT package. We modified three of these rate constants from their BCT v4.2 default values to incorporate our recent measurements. Specifically, we set $k = 50\ \mu M^{-1}\ s^{-1}$ as the second-order rate constant for CheA → CheY phosphotransfer and $k = 12\ \mu M^{-1}\ s^{-1}$ for CheA → CheB phosphotransfer reactions involving wild-type CheA (*25*, *26*, and Stewart et al., in preparation), and we used values of 1.5 and 0.35 $\mu M^{-1}\ s^{-1}$ for the respective phosphotransfer reactions in BCT simulations involving CheAΔP2 (values determined in this work). In addition, we modified the rate constant for CheZ-mediated dephosphorylation of P-CheY from the default value (0.126 $\mu M^{-1}\ s^{-1}$) to 0.22 $\mu M^{-1}\ s^{-1}$. This modification was necessary to obtain a steady-state P-CheY concentration close to the level estimated for unstimulated, wild-type *E. coli* (*43*), and it brings this rate constant into agreement with our previous measurements (*44*). Our simulations used the BCT default values for the Che protein and Tar concentrations.

To calculate flagellar rotation bias for any given level of P-CheY (Figure 6B), we made use of the relationship defined by Cluzel et al. (*45*): CW bias $= [\text{P-CheY}]^N/([\text{P-CheY}]^N + K_d^N)$. This is a version of the Hill equation where N is the Hill coefficient and K_d is the dissociation constant for the complex formed between P-CheY and the flagellar motor. For these calculations, we used the N value (10.3) and K_d value (3.1 μM) reported by Cluzel et al. (*45*).

RESULTS

Properties of CheAΔP2. Details of the construction and characterization of the CheAΔP2 protein will be described elsewhere (Jahreis et al., in preparation). In essence, we removed the P2 coding region and joined the flanking L1 and L2 segments with a proline- and alanine-rich linker, as depicted in Figure 1. The mutant protein was purified by the same procedure as wild-type CheA and was found to autophosphorylate at approximately the same rate as wild-type CheA (data not shown). On mixing ^{32}P-CheAΔP2 with CheY, we observed complete transfer of the labeled phosphoryl group to CheY within 5 s, the fastest time point we could achieve by manually mixing the reactants and then quenching the reaction with SDS−PAGE sample buffer. This initial test demonstrated that phosphotransfer from CheAΔP2 to CheY was too rapid to distinguish from the corresponding wild-type CheA reaction using manual mixing experiments. Consequently, we turned to the rapid reaction instruments used in earlier studies to characterize phosphotransfer from wild-type CheA to CheY (*25*, *26*).

Measurements of CheAΔP2 Phosphotransfer Kinetics. We used quenched-flow and stopped-flow approaches to monitor the time course of phosphotransfer from P-CheAΔP2 to CheY. Both types of experiments were performed under pseudo-first-order conditions, i.e., with the CheY phosphoacceptor in at least 10-fold molar excess over the P-CheAΔP2 phosphodonor, and the reactions were sampled over a time course of 5−5000 ms. In the quenched-flow experiments, the phosphodonor was ^{32}P-CheAΔP2, enabling us to follow the appearance of the label in CheY and its concomitant disappearance from CheAΔP2. At each time point, samples were mixed with SDS and EDTA to stop the phosphotransfer reaction, and the levels of ^{32}P-CheAΔP2 and ^{32}P-CheY were determined. Representative results are shown in Figure 2. In the stopped-flow experiments, we followed the intrinsic fluorescence of the reactants to monitor the course of the reaction. CheY fluorescence decreases upon CheY phosphorylation (*15*), whereas CheA fluorescence is not sensitive to CheA phosphorylation state (Stewart, unpublished observation). Representative results from the stopped-flow experiments are shown in Figure 3.

Rate measurements from the two experimental approaches were in excellent agreement. Each time course was fit well

[2] In addition to phosphorylating CheY, CheA also directs phosphorylation of CheB (*4*). Our unpublished results indicate that the rate of phosphotransfer from P-CheAΔP2 to CheB is 30−40-fold slower than the corresponding reaction with wild-type CheA. This effect was included in the BCT simulations.

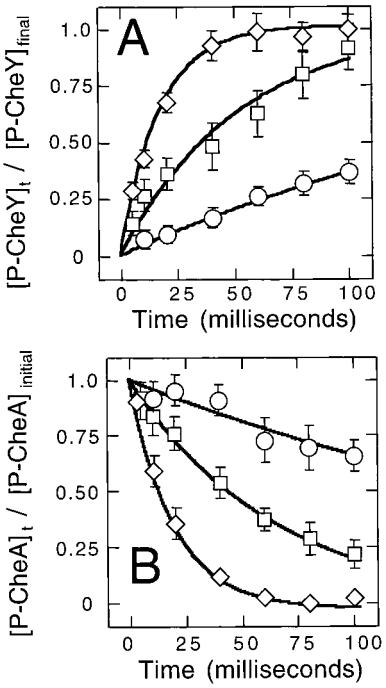

FIGURE 2: Time course of phosphotransfer from CheAΔP2 to CheY. ^{32}P-CheAΔP2 (0.25 μM after mixing) was mixed with excess CheY in a rapid-quench instrument, and the phosphotransfer reaction was allowed to proceed for the indicated times before quenching (with SDS and EDTA). Levels of ^{32}P-CheAΔP2 and ^{32}P-CheY were determined as described in Experimental Procedures. Each data point represents the average of two replicates for a single experiment: 2.5 μM CheY (○); 10 μM CheY(□); 40 μM CheY (◇). Concentrations given here are the postmixing values. Panel A: appearance of ^{32}P-CheY. Panel B: disappearance of ^{32}P-CheA. The plots show just the first 100 ms of time courses that were carried out to 5000 ms. The final level of phosphorylated CheY was not affected by the CheY concentration in this range (i.e., $[\text{P-CheY}]_{\text{final}}$ was ~0.25 μM for each experiment), indicating quantitative transfer of the phosphoryl group from CheA to CheY. Solid lines represent computer-generated best fits of the data to a single exponential, and the first-order rate constants derived from such least-squares fits were defined as k_{obsd} values. Error bars indicate standard errors of the mean.

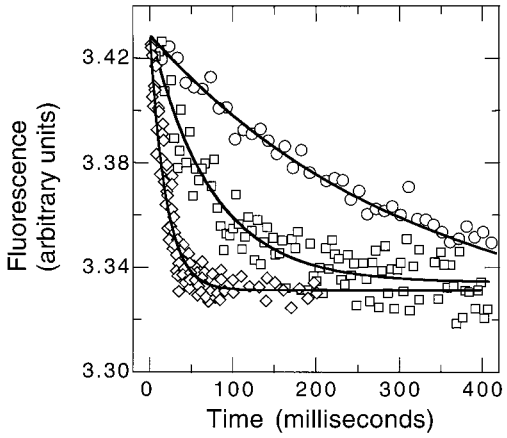

FIGURE 3: Time course of fluorescence changes following mixing of P-CheAΔP2 with CheY. P-CheAΔP2 (0.25 μM) was mixed with 2.5 μM CheY (○), 10 μM CheY (□), or 40 μM CheY (◇), and the rapid decrease in fluorescence emission intensity was monitored. Concentrations listed here are the postmixing values. Each data set represents the average of at least 10 consecutive stopped-flow shots. Solid lines represent computer-generated best fits of the data to a single exponential, and the first-order rate constants derived from such least-squares fits were defined as k_{obsd} values. When time courses were extended to longer times (e.g., out to 20 s), a slow increase in fluorescence signal ($k_{\text{obsd}} = 0.04\ \text{s}^{-1}$) followed the rapid changes shown in the figure, as expected for the CheY autodephosphorylation reaction (*16*, *26*). Note that the experimental conditions resulted in phosphorylation of only a small fraction of the total CheY present in the reaction mixtures (10% for 2.5 μM CheY; 0.25% for 40 μM CheY). Therefore, the decreases in signal intensity due to CheY phosphorylation were observed on top of a large, constant background signal due to the unphosphorylated CheY. Because the concentration of CheY is different for the three time courses shown in the figure, the magnitude of this background signal was different. To facilitate comparison of these time courses, the 2.5 and 10 μM CheY time courses are shifted up along the *y*-axis such that the fluorescence intensities at their starting points matched that of the 40 μM time course.

by a single exponential (Figures 2 and 3), and such fits were used to extract the pseudo-first-order rate constant (k_{obsd}) for reactions run at CheY concentrations ranging from 1 to 50 μM. Both methods yielded essentially identical k_{obsd} values at any particular CheY concentration (Figure 4). Moreover, both sets of k_{obsd} values showed a first-order dependence on CheY concentration with no evidence of rate saturation at the highest CheY levels tested (Figure 4). In contrast, phosphotransfer from wild-type CheA exhibits saturation kinetics, with a K_{m} of approximately 7 μM (*25*). Thus, the phosphotransfer reaction from CheAΔP2 is either rate-limited by collisional interactions between the phosphodonor and phosphoacceptor or else involves a binding interaction only evident at very high, i.e., nonphysiological, reactant concentrations.

Phosphotransfer from CheA$^{1-139}$ to CheY. Although CheAΔP2 lacks the high-affinity CheY-docking domain, it retains the kinase catalytic domain, the C-terminal regulatory domain, and various linker regions of the full-length protein (Figure 1). It is conceivable that any of these remaining segments might (i) influence the ability of the phosphorylated P1 domain of CheAΔP2 to interact with CheY or (ii) influence phosphotransfer kinetics by interacting directly with CheY in unanticipated ways. To examine such possibilities, we used stopped-flow fluorescence measurements to monitor phosphotransfer from an isolated P1 domain (CheA$^{1-139}$) to CheY. These results (Figure 4, triangles) indicated that the kinetics of CheY phosphorylation by P-CheA$^{1-139}$ are very similar to those observed for CheY phosphorylation by P-CheAΔP2. We conclude that the kinetics of phosphotransfer from P-CheAΔP2 to CheY reflect the interaction of CheY with the phosphorylated P1 domain of P-CheAΔP2 and that this interaction is not affected significantly by the kinase domain, the regulatory domain, or the linker regions of CheAΔP2.

Phosphotransfer Effects of P1 and P2 Domains in trans. Our kinetic measurements showed that phosphotransfer to CheY from P-CheAΔP2 was considerably slower than it is from wild-type CheA. For example, at a CheY concentration of 10 μM, phosphotransfer from wild-type CheA is more than 25-fold faster ($k_{\text{obsd}} \sim 400\ \text{s}^{-1}$ vs $k_{\text{obsd}} \sim 15\ \text{s}^{-1}$). If binding of CheY to the P2 module of CheA places CheY in a conformation that facilitates the phosphotransfer reaction, it might be possible to enhance phosphotransfer from CheAΔP2 by supplying the P2 domain in *trans*. Using stopped-flow fluorescence experiments, we examined the reaction of CheY with P-CheAΔP2 in the presence of varying concentrations of CheA$^{124-257}$, a CheA fragment encompassing the P2 domain (*31*, *36*) and its CheY binding site (*29*, *32*) (see Figure 1). As shown in Figure 5A, the CheA$^{124-257}$

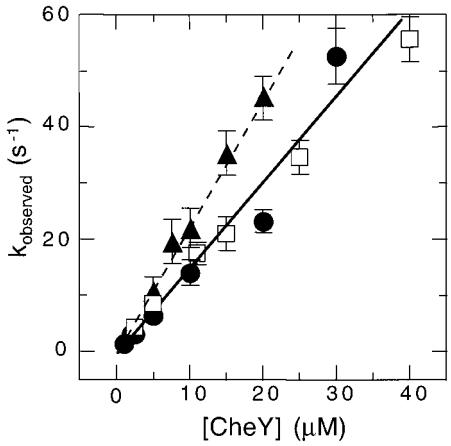

FIGURE 4: Analysis of the effect of CheY concentration on the kinetics of phosphotransfer from P-CheAΔP2 to CheY and from P-CheA$^{1-139}$ to CheY. For the reaction between CheY and P-CheAΔP2, the plotted k_{obsd} values are the pseudo-first-order rate constants derived from rapid quench (□) and stopped-flow (●) experiments (as in Figures 2 and 3). The best-fit linear relationship defined in this plot (solid line) indicates a second-order rate constant of 1.5×10^6 M^{-1} s^{-1} for the reaction between CheY and P-CheAΔP2. For the reaction between CheY and P-CheA$^{1-139}$, the plotted k_{obsd} values (▲) were determined by stopped-flow experiments. The best linear fit (dashed line) of these data indicates a second-order rate constant of 2.3×10^6 M^{-1} s^{-1}. Error bars indicate standard errors of the mean.

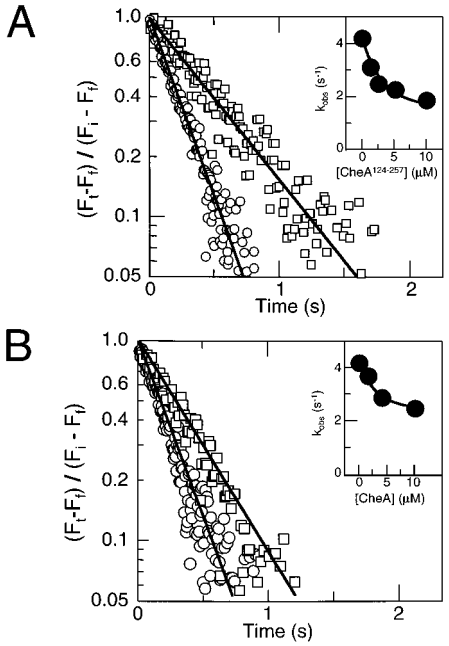

FIGURE 5: Effect of CheA$^{124-257}$ and wild-type CheA on the rate of phosphotransfer from CheAΔP2 to CheY. Panel A: reaction mixtures contained 0.25 μM P-CheAΔP2, 2.8 μM CheY, and either no CheA$^{124-257}$ (○) or 10 μM CheA$^{124-257}$ (□). The inset shows the relationship between the observed first-order rate constant (k_{obsd}) and the concentration of CheA$^{124-257}$. Panel B: reaction mixtures contained 0.25 μM P-CheAΔP2, 2.8 μM CheY, and either no wild-type CheA (○) or 10 μM wild-type CheA (□). The inset shows the relationship between the observed first-order rate constant (k_{obsd}) and the concentration of CheA. In both panels, reaction time courses were monitored using fluorescence emission changes as in Figure 3. The data are presented as normalized semilog plots because the reactions in the presence of CheA$^{124-257}$ or wild-type CheA exhibited smaller amplitudes than did reactions in the absence of these additions [as expected because of the quenching of CheY intrinsic fluorescence associated with CheY binding to the P2 module of CheA (*38*)]. F_i, F_t, and F_f denote the fluorescence emission intensity observed at $t = 0$, $t =$ time t, and at the end point of the reaction, respectively. The solid lines in the main panels represent the computer-generated best fits of each time course to a single exponential. The solid lines in the insets depict the inhibition pattern expected if the CheY·P2 complex has a K_d of 1.5 μM and a phosphotransfer activity that is 30% that of free CheY.

polypeptide actually caused a small but reproducible *inhibition* of the rate of phosphotransfer from P-CheAΔP2 to CheY. Thus, the P2 module present in CheA$^{124-257}$ does not appear to be capable of enhancing phosphotransfer from a P1 module in *trans*. Instead, binding of CheY to CheA$^{124-257}$ appears to render CheY less capable of interacting with P-CheAΔP2. Although such an effect seems counterintuitive because it would reduce signaling efficiency in vivo, we previously observed a similar inhibitory effect of CheA$^{124-257}$ on CheY phosphorylation by small molecule phosphodonors such as acetyl phosphate and phosphoramidate (*26*).

A substantial portion of the CheY molecule is known to undergo subtle conformational change upon binding to the P2 module (*21*, *22*, *46*). Our results might reflect a decreased phosphoaccepting ability for CheY in this altered, P2-bound conformation. However, we note that CheA$^{124-257}$ includes, in addition to the P2 domain, a small fragment of the P1 domain and two linker regions, as shown in Figure 1. This raises the possibility of an alternative explanation for the negative effect of CheA$^{124-257}$: perhaps these regions flanking P2 in CheA$^{124-257}$ are responsible for the observed inhibition and/or mask an accelerating influence by the P2 module. Distinguishing between these alternative interpretations will require further experiments using an isolated P2 peptide that lacks the flanking regions present in CheA$^{124-257}$.

To accomplish phosphotransfer, CheY must interact with the phosphorylated P1 module of wild-type P-CheA (or P-CheAΔP2). This interaction must, of course, involve the phosphorylated His^{48} side chain of P1 but might involve additional binding contacts between CheY and P1. If so, an unphosphorylated P1 module might inhibit phosphotransfer from P-CheAΔP2 to CheY by sequestering CheY. To test that possibility, we examined P-CheAΔP2 phosphotransfer kinetics in the presence of increasing concentrations of unphosphorylated CheAΔP2 (0−25 μM). Even at the highest concentrations tested, unphosphorylated CheAΔP2 had no effect on the rate of the phosphotransfer reaction (results not shown). This result indicates that the affinity of any binding interaction between P1 and CheY must be quite weak (e.g., at least 25 times weaker than the affinity of CheY for phospho-P1).

We also explored the possibility that binding of CheY to unphosphorylated wild-type CheA could inhibit the ability of CheY to interact with P-CheAΔP2. The underlying rationale for this experiment was that unphosphorylated P1 might be an effective inhibitor when tethered to the P2 domain in the context of full-length CheA. Such tethering might, for example, expose CheY to a high effective "local concentration" of P1, and this high local concentration of unphosphorylated P1 might inhibit CheY's ability to interact with the phosphorylated P1 module of P-CheAΔP2. As shown in Figure 5B, wild-type CheA did inhibit phosphotransfer from P-CheAΔP2 to CheY. However, the extent of this inhibition was similar to that caused by CheA$^{124-257}$ (Figure 5A). We conclude that the inhibition observed with wild-type CheA (Figure 5B) resulted from conformational

alteration of CheY caused by binding to P2 rather than from any enhanced ability of P1 to interact with CheY in the context of full-length CheA.

DISCUSSION

In previous work, we demonstrated that phosphorylation of CheY by wild-type CheA takes place on a millisecond time scale (*25*, *26*). We are interested in defining the features of CheY and CheA that contribute to the speed of this phosphotransfer reaction. Because it contains a high-affinity binding site for CheY, the P2 domain of CheA is likely to make important contributions (*29*, *32*). In the work reported here, we explored the role of this domain in the kinetics of CheA → CheY phosphotransfer. Our results indicate that phosphorylation of CheY by CheAΔP2 is considerably slower than is CheY phosphorylation by wild-type CheA. Below we consider the significance of this observation at two levels: first, how the altered phosphotransfer kinetics are expected to influence the overall operation of the chemotaxis system, and second, what our results reveal about the molecular mechanism of CheA → CheY phosphotransfer.

Importance of Rapid Phosphotransfer for Chemotaxis Signaling. Using CheY and CheA at their approximate in vivo concentrations [10−20 and 1−5 μM, respectively *(40)*], we observed a pseudo-first-order rate constant of 15−30 s^{-1} with P-CheAΔP2 compared to a value of 400−600 s^{-1} for phosphorylated wild-type CheA. Would this rate difference affect the intracellular level of P-CheY, and if so, would this alter the cell's ability to execute chemotaxis responses? To address these questions, we performed computer simulations (described in Experimental Procedures) using the BCT program developed by Bray and Bourret (*40*, *41*). This program describes the chemotaxis signaling circuitry as a set of differential equations and can calculate the P-CheY level in unstimulated cells. In addition, BCT can simulate how this level changes when a cell encounters a chemotactic stimulus. We used this program to examine the possible effects of altering the rate constant (k_{phos}) for the CheA → CheY phosphotransfer reaction.[2] In particular, we explored how the value of k_{phos} affects the steady-state concentration of P-CheY before and after subjecting the system to a hypothetical test stimulus (removal of chemoattractant, 3 μM aspartate). As shown in Figure 6A, these simulations indicate that both the prestimulus level of P-CheY ($[P\text{-}CheY]_{unstim}$) and the magnitude of the stimulus-induced increase in P-CheY ($\Delta[P\text{-}CheY]_{stim}$) are affected by the value of k_{phos}, especially in the range where the ratio of the hypothetical k_{phos} to the k_{phos} of wild-type CheA falls between 0 and 0.1. Using the k_{phos} values we measured for CheAΔP2 (∼1.5 μM^{-1} s^{-1}) and for wild-type CheA[3] (∼50 μM^{-1} s^{-1}), Figure 6A indicates that, compared to wild-type CheA, CheAΔP2 would give rise to a lower value of $[P\text{-}CheY]_{unstim}$ (2.0 versus 2.75 μM) and to a diminished response magnitude ($\Delta[P\text{-}CheY]_{stim}$ is 0.7 μM for CheAΔP2 versus 1.5 μM for wild-type CheA).

[3] BCT calculates the rate of the CheA → CheY phosphotransfer reaction as k_{phos}[CheY][P-CheA]. Our previous work (*25*, *26*) indicates that the rate of phosphotransfer does not exhibit a strict first-order dependence on [CheY] but rather exhibits saturation kinetics ($K_m \sim 7$ μM and $k_{cat} \sim 750$ s^{-1}). On the basis of our measurements, when [CheY] is in the range between 5 and 10 μM CheY, the reaction rate can be approximated by the BCT relationship using $k_{phos} \sim 50$ μM^{-1} s^{-1}.

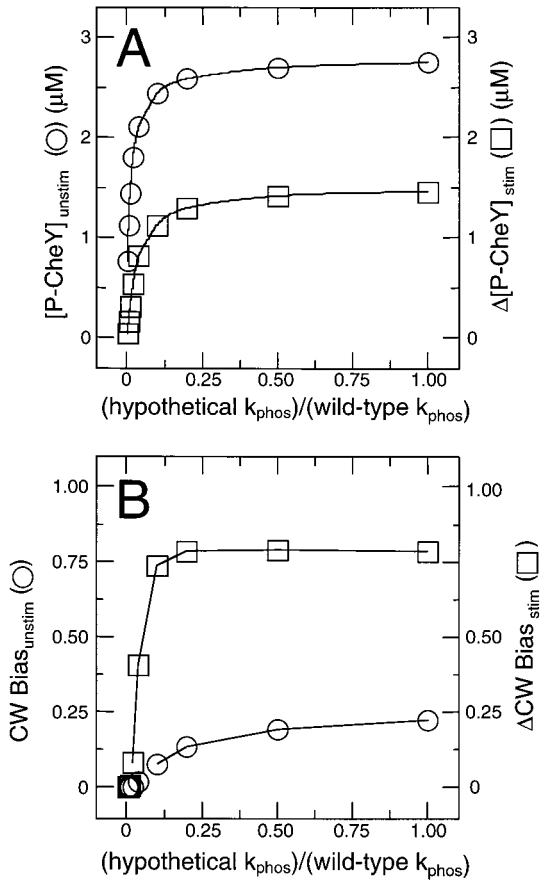

FIGURE 6: Computer-modeled relationship of the effect of the phosphotransfer rate constant (k_{phos}) on the intracellular level of P-CheY and on the flagellar CW rotation bias. Computer simulations were performed using the BCT v4.2 program of Bourret and Bray (*40*, *41*) as described in Experimental Procedures. For these simulations the rate constants for CheA → CheY and CheA → CheB phosphotransfer[2] were varied in parallel by multiplying their wild-type values (50 and 0.22 μM^{-1} s^{-1}) by a common factor indicated as (hypothetical k_{phos})/(wild-type k_{phos}). Panel A: for each set of k_{phos} values, a BCT simulation was performed to calculate the expected steady-state level of P-CheY before and after a hypothetical stimulus (removal of 3 μM aspartate). Plotted are the prestimulus P-CheY concentration (○) and the predicted stimulus-induced change in P-CheY concentration (□). Panel B: the prestimulus and poststimulus P-CheY levels shown in panel A were used to calculate the anticipated CW rotation bias of flagella (i.e., the fraction of time that a flagellar motor spends rotating in the CW direction) using the Hill equation and parameters defined by Cluzel et al. (*45*). Plotted are the prestimulus bias (○) and the predicted stimulus-induced change in bias (□). The lines in both panels serve only to connect the data points and have no theoretical significance.

Would these changes affect the chemotaxis ability of *E. coli*? Answering this question requires a qualitative understanding of the role of P-CheY in chemotaxis signaling and a detailed quantitative understanding of the relationship between [P-CheY] and the cell swimming pattern. In the absence of chemostimuli, *E. coli* alternates frequently between periods of smooth swimming [1−2 s "runs" that result from counterclockwise (CCW) flagellar rotation] and briefer episodes of "tumbling" [0.1−0.2 s periods of somersaulting that result from clockwise (CW) flagellar rotation and serve to change the swimming direction of the cell] (*1*). To accomplish chemotaxis, a cell modulates the frequency of tumbling episodes (i.e., the probability of CW flagellar rotation) (*47*). This modulation is reflected in the CW bias of the flagellar motors (i.e., the fraction of time

that a motor spends rotating in the CW direction): in the absence of chemostimuli, the flagellar motors exhibit a CW bias of 0.14−0.36, and this rapidly increases to a bias of ~1 when cells encounter a strong CheA-activating stimulus, such as decreased [attractant] that changes the ligand-binding state of >50% of the receptors (*23*, *43*, *47*). The bias of the flagellar motors at any given time is determined by the intracellular concentration of P-CheY (*43*). P-CheY binds to the switch components of the motor and promotes CW flagellar rotation; unphosphorylated CheY does not interact with the motor in this manner and so allows it to operate in its default mode, CCW (*48*, *49*). By regulating the concentration of P-CheY, the chemotaxis system modulates the CW bias of the motors and so controls the cell swimming pattern.

The quantitative relationship between P-CheY concentration and the CW bias of flagellar rotation has been investigated intensively (*43*, *45*, *50*). We used the relationship defined by Cluzel et al. (*45*) to estimate the CW motor bias expected for each value of $[\text{P-CheY}]_{\text{unstim}}$ in Figure 6A and to calculate the predicted change in bias associated with each $\Delta[\text{P-CheY}]_{\text{stim}}$. As shown in Figure 6B, these calculations indicate that low values of k_{phos}, such as that observed with CheAΔP2, are predicted to cause a large decrease in the CW bias of motors in unstimulated cells and to diminish the magnitude of the response (bias change) generated following a CheA-activating stimulus. For example, Figure 6B predicts a bias change of ~0.3 for CheAΔP2 compared to a value of ~0.78 for wild-type CheA for responses to our test stimulus (removal of 3 μM aspartate). This analysis predicts that a cell expressing *cheAΔP2* in place of wild-type *cheA* would tumble infrequently in the absence of chemostimuli and would be impaired with respect to its ability to respond to chemostimuli. These behavioral predictions have been confirmed experimentally (Jahreis et al., in preparation). The loss of chemotaxis ability in *cheAΔP2* cells appears to arise solely from the reduced phosphotransfer activity of CheAΔP2. Other activities (including autokinase activity and modulation of this activity by the chemotaxis receptors) appear to be normal for this CheA variant (Jahreis et al., in preparation), so its failure to support efficient chemotaxis is evidently due to the reduction in the rate of CheA → CheY phosphotransfer.

Contributions of P2 and P1 to Rapid CheA → CheY Phosphotransfer. Given the critical importance of phosphotransfer speed to effective chemotaxis signaling, how do CheA and CheY accomplish this reaction on a rapid time scale? Note that the relative catalytic efficiencies of CheY phosphorylation by wild-type CheA ($k_{\text{phos}} = k_{\text{cat}}/K_{\text{m}} \sim 10^8$ $\text{M}^{-1}\ \text{s}^{-1}$) and by CheAΔ*P2* ($k_{\text{phos}} \sim 1.5 \times 10^6\ \text{M}^{-1}\ \text{s}^{-1}$) are very much greater than by small molecule phosphodonors ($k_{\text{phos}} \sim 5-50\ \text{M}^{-1}\ \text{s}^{-1}$) (*16*, *26*, *51*). If CheY phosphorylation in these three situations (depicted in Figure 7) involves the same basic chemical events, as seems likely, then the low k_{phos} value seen with small molecule phosphodonors indicates that the chemistry of His → Asp phosphotransfer is not inherently fast. Therefore, features of CheA have evolved to accelerate these events. Our results suggest that both the P2 domain and the P1 domain of CheA make important contributions to this acceleration.

The dramatic effect of the P2 deletion on the K_{m} of the CheA → CheY phosphotransfer reaction indicates that P2 provides the high-affinity binding site utilized by CheY

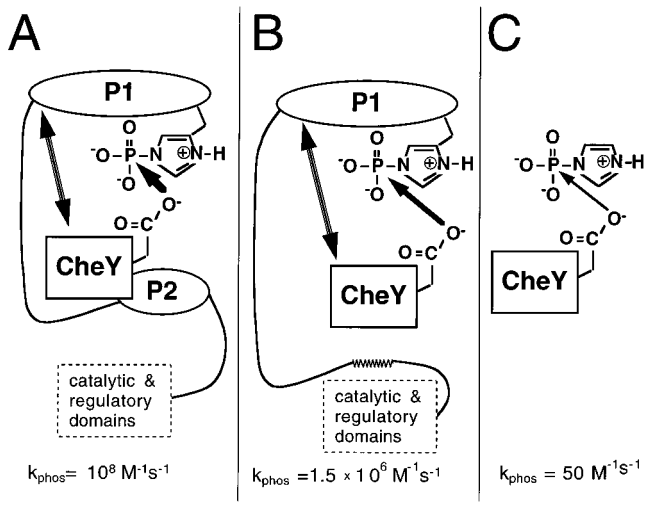

FIGURE 7: Model depicting the roles of the P1 and P2 domains of CheA in the CheA → CheY phosphotransfer reaction. Panel A shows CheY interacting with phosphorylated wild-type CheA. Binding to the P2 domain of CheA tethers CheY in close proximity to the phosphohistidine side chain provided by P1. This promotes phosphotransfer by providing a high local concentration of phosphodonor to Asp^{57} of CheY. Interactions between CheY and the P1 domain (indicated by the double-headed arrow) also enhance the rate of phosphotransfer. Panel B shows CheY interacting with P-CheAΔP2. The absence of the P2 docking site slows the rate of phosphotransfer somewhat, but interactions between CheY and P1 are still present and facilitate phosphotransfer. Panel C depicts CheY interacting with phosphoimidazole. In the absence of the accelerating interactions with P1 and P2, this phosphotransfer reaction is very slow. k_{phos} is the effective second-order rate constant for CheY phosphorylation. The indicated values are from work reported here (Figure 4), from our previous work (*25*, *26*), and from our extrapolation of work published by Silversmith et al. (*16*). Phosphohistidine (phosphoimidazole) is shown in a protonated state to account for the pH dependence of the phosphotransfer reaction (*16*).

during its interactions with phosphorylated wild-type CheA. Moreover, binding of CheY to P2 takes place extremely rapidly ($k_{\text{on}} \sim 10^{10}\ \text{M}^{-1}\ \text{s}^{-1}$) (Stewart, unpublished results), suggesting that P2 provides a mechanism for rapid association of CheY with its phosphodonor. Thus, P2 could conceivably contribute to the kinetics of phosphotransfer either by inducing a conformational change in CheY that enhances its ability to acquire the phosphoryl group from P-CheA or by effectively tethering CheY in a region of high "local concentration" of the phosphorylated P1 domain. Our analysis of the kinetics of CheY phosphorylation by P-CheAΔP2 and by wild-type P-CheA indicates that P2 contributes to the rate of phosphotransfer via the second of these mechanisms but probably not the first.

Binding of CheY to P2 is known to alter the structure of the "acid pocket" that serves as the CheY active site (*21*, *22*, *46*). However, we found that P2 domains in *trans* could not enhance the phosphoacceptor activity of CheY, indicating that P2-induced conformational changes of the CheY active site probably do not contribute significantly to the kinetics of CheA → CheY phosphotransfer. By contrast, in a *cis* configuration P2 could contribute to the rate of phosphotransfer by tethering CheY in close proximity to phosphorylated His^{48} in the covalently connected P1 domain (as depicted in Figure 7A). This tethering could, for example, position Asp^{57} immediately adjacent to P-His^{48} in an active site arrangement that would enhance the rate of phosphotransfer by dramatically increasing the "effective local

concentrations" of the phosphodonor and phosphoacceptor. By comparing the second-order rate constant for CheAΔP2 (1.5×10^6 M^{-1} s^{-1}) to the k_{cat} value ($\sim$750 s^{-1}) for the wild-type CheA reaction, we calculate that tethering results in an effective local concentration of $\sim$500 μM phospho-P1 available to CheY. This effective concentration is quite small compared to the enormous values (10^1-10^8 M) observed in various model systems designed to mimic enzyme active sites (*52*, *53*). This comparison suggests that tethering of CheY to the P2 domain of P-CheA does not constrain the reactants (Asp^{57} of CheY and P-His^{48} of P1) to the extent expected for an active site. A simple calculation suggests that the observed effective concentration of phospho-P1 could be accounted for by constraining Asp^{57} and P-His^{48} to the volume occupied by a sphere with a radius of $\sim$90 Å. NMR studies of $CheA^{1-233}$ indicate that P1 and P2 are distinct, noninteracting structural domains joined by a 24 amino acid linker (*30*) that serves as a flexible hinge to allow P1 and P2 to move independently (*31*). If this linker adopts a random coil conformation, then the average distance separating the C-terminal end of P1 from the N-terminal end of P2 would be $\sim$60 Å (*54*), a distance that, based on the structure of Zhou et al. (*18*), could easily accommodate a 90 Å separation between His^{48} in the P1 domain of CheA and Asp^{57} of CheY bound to the P2 domain of CheA. Therefore, our results suggest that the kinetic effect of tethering CheY to P2 can be accounted for without limiting the relative movements of P1 and P2. This observation argues against models in which P2 serves as a scaffolding that arranges Asp^{57} and phospho-His^{48} in close proximity in an active site.

Although slower than the reaction of CheY with phosphorylated wild-type CheA, phosphorylation of CheY by P-CheAΔP2 is quite fast compared to CheY phosphorylation by phosphoimidazole and other small molecule phosphodonors. The 10^4-10^5-fold difference in k_{phos} suggests that the P1 domain of CheA makes significant contributions to the rate of phosphotransfer. P1 might contribute to the rate of phosphotransfer (i) by providing a transient docking site for CheY (*35*), (ii) by providing catalytic groups that promote specific events (such as charge redistribution) during phosphotransfer (*16*, *55*, *56*), or (iii) by providing an environment of low dielectric constant in which the phosphotransfer chemistry would take place more rapidly (*26*). The nature of CheY's interactions with P1 remains obscure. We presume that specific contact points are involved, but our experiments do not provide direct evidence of a discrete CheY·P1 complex, suggesting that the CheY $\leftrightarrow$ P1 interaction is weak and short-lived. We have isolated mutations in P1 that appear to slow the rate of P1 $\rightarrow$ CheY phosphotransfer. We anticipate that characterization of these mutants will help to define features of P1 that facilitate its rapid interaction with CheY.

REFERENCES

1. Macnab, R. M. (1996) in *Escherichia coli and Salmonella: Cellular and Molecular Biology* (Neidhardt, F. C., Curtiss, R., Ingraham, J. L., Lin, E. C. C., Low, K. B., Maganasanik, B., Reznikoff, W. S., Riley, M., Schaechter, M., and Umbarger, H. E., Eds.) pp 123−145, ASM Press, Washington, DC.
2. Stock, J., and Surette, M. G. (1996) in *Escherichia coli and Salmonella: Cellular and Molecular Biology* (Neidhardt, F. C., Curtiss, R., Ingraham, J. L., Lin, E. C. C., Low, K. B., Maganasanik, B., Reznikoff, W. S., Riley, M., Schaechter, M., and Umbarger, H. E., Eds.) pp 1103−1129, ASM Press, Washington, DC.
3. Hess, J. F., Bourret, R. B., and Simon, M. I. (1988) *Nature 336*, 139−143.
4. Hess, J. F., Oosawa, K., Kaplan, N., and Simon, M. I. (1988) *Cell 53*, 79−87.
5. Borkovich, K. A., Kaplan, M., Hess, J. F., and Simon, M. I. (1989) *Proc. Natl. Acad. Sci. U.S.A. 86*, 1208−1212.
6. Borkovich, K. A., and Simon, M. I. (1990) *Cell 63*, 1339−1348.
7. Ninfa, E. G., Stock, A., Mowbray, S., and Stock, J. (1991) *J. Biol. Chem. 266*, 9764−9770.
8. Levit, M., Liu, Y., and Stock, J. B. (1999) *Biochemistry 38*, 6651−6658.
9. Welch, M., Oosawa, K., Aizawa, S.-I., and Eisenbach, M. (1994) *Biochemistry 33*, 10470−10476.
10. Barak, R., and Eisenbach, M. (1996) *Curr. Top. Cell Regul. 34*, 137−158.
11. Robinson, V. L., and Stock, A. M. (1999) *Structure 7*, R47−R53.
12. Parkinson, J. S., and Kofoid, E. C. (1992) *Annu. Rev. Genet. 26*, 71−112.
13. Hoch, J., and Silhavy, T., Eds. (1995) *Two-Component Systems*, ASM Press, Washington, DC.
14. Sanders, D. A., Gillece-Castro, B. L., Stock, A. M., Burlingame, A. L., and Koshland, D. E., Jr. (1989) *J. Biol. Chem. 264*, 21770−21778.
15. Lukat, G. S., McCleary, W. R., Stock, A. M., and Stock, J. B. (1992) *Proc. Natl. Acad. Sci. U.S.A. 89*, 718−722.
16. Silversmith, R. E., Appleby, J. L., and Bourret, R. B. (1997) *Biochemistry 36*, 14965−14974.
17. Bilwes, A. A., Alex, L. A., Crane, B. R., and Simon, M. I. (1999) *Cell 96*, 131−141.
18. Zhou, H., Lowry, D. F., Swanson, R. V., Simon, M. I., and Dahlquist, F. W. (1995) *Biochemistry 34*, 13858−13870.
19. Stock, A. M., Martinez-Hackert, E., Rasmussen, B. F., West, A. H., Stock, J. B., Ringe, D., and Petsko, G. (1993) *Biochemistry 32*, 13375−13380.
20. Volz, K., and Matsumura, P. (1991) *J. Biol. Chem. 266*, 15511−15519.
21. McEvoy, M. M., Hausrath, A. C., Randolph, G. B., Remington, S. J., and Dahlquist, F. W. (1998) *Proc. Natl. Acad. Sci. U.S.A. 95*, 7333−7338.
22. Welch, M., Chinardet, N., Mourey, L., Birck, C., and Samama, J. (1998) *Nat. Struct. Biol. 5*, 25−29.
23. Block, S. M., Segall, J. E., and Berg, H. C. (1982) *Cell 31*, 215−226.
24. Jasuja, R., Keyoung, J., Reid, G. P., Trentham, D. R., and Khan, S. (1999) *Biophys. J. 76*, 1706−1719.
25. Stewart, R. C. (1997) *Biochemistry 36*, 2030−2040.
26. Mayover, T. L., Halkides, C. J., and Stewart, R. C. (1999) *Biochemistry 38*, 2259−2271.
27. Fisher, S. L., Kim, S. K., Wanner, B. L., and Walsh, C. T. (1996) *Biochemistry 35*, 4732−4740.
28. Jin, S., Prasti, R. K., Roitsch, T., Ankenbauer, R. G., and Nester, E. W. (1990) *J. Bacteriol. 172*, 4945−4950.
29. Swanson, R. V., Schuster, S. C., and Simon, M. I. (1993) *Biochemistry 32*, 7623−7629.
30. Morrison, T. B., and Parkinson, J. S. (1997) *J. Bacteriol. 179*, 5543−5550.
31. Zhou, H., McEvoy, M. M., Lowry, D. F., Swanson, R. V., Simon, M. I., and Dahlquist, F. W. (1996) *Biochemistry 35*, 433−443.
32. Li, J., Swanson, R. V., Simon, M. I., and Weis, R. M. (1995) *Biochemistry 34*, 14626−14636.
33. Wolfe, A. J., Macnamara, B. P., and Stewart, R. C. (1994) *J. Bacteriol. 176*, 4483−4491.
34. Smith, R. A., and Parkinson, J. S. (1980) *Proc. Natl. Acad. Sci. U.S.A. 77*, 5370−5374.
35. Garzon, A., and Parkinson, J. S. (1996) *J. Bacteriol. 178*, 6752−6758.
36. Morrison, T. B., and Parkinson, J. S. (1994) *Proc. Natl. Acad. Sci. U.S.A. 91*, 5485−5489.

37. Gill, S. C., and von Hippel, P. H. (1989) *Anal. Biochem. 182*, 319−326.
38. McEvoy, M. M., Zhou, H., Roth, A. F., Lowry, D. F., Morrison, T. M., Kay, L. E., and Dahlquist, F. W. (1995) *Biochemistry 34*, 13871−13880.
39. Levit, M., Liu, Y., Surette, M., and Stock, J. (1996) *J. Biol. Chem. 271*, 32057−32063.
40. Bray, D., Bourret, R. B., and Simon, M. I. (1993) *Mol. Biol. Cell 4*, 469−482.
41. Bray, D., and Bourret, R. B. (1995) *Mol. Biol. Cell 6*, 1367−1380.
42. Mowbray, S. L., and Koshland, D. E., Jr. (1990) *J. Biol. Chem. 265*, 15638−15643.
43. Alon, U., Camarena, L., Surette, M. G., Aguera y Arcas, B., Liu, Y., Leibler, S., and Stock, J. B. (1998) *EMBO J. 17*, 4238−4248.
44. Huang, C., and Stewart, R. C. (1993) *Biochim. Biophys. Acta 1201*, 297−304.
45. Cluzel, P., Surette, M., and Leibler, S. (2000) *Science 287*, 1652−1655.
46. Swanson, R., Lowry, D. F., Matsumura, P., McEvoy, M. M., Simon, M. I., and Dahlquist, F. W. (1995) *Nat. Struct. Biol. 2*, 906−910.
47. Berg, H. C., and Brown, D. A. (1972) *Nature 239*, 500−504.
48. Welch, M., Oosawa, K., Aizawa, S.-I., and Eisenbach, M. (1993) *Proc. Natl. Acad. Sci. U.S.A. 90*, 8787−8791.
49. Welch, M., Oosawa, K., Aizawa, S.-I., and Eisenbach, M. (1994) *Biochemistry 33*, 10470−10476.
50. Scharf, B. E., Fahner, K. A., Turner, L., and Berg, H. C. (1998) *Proc. Natl. Acad. Sci. U.S.A. 95*, 201−206.
51. Da Re, S. S., Deville-Bonne, D., Tolstykh, T., Beron, M., and Stock, J. B. (1999) *FEBS Lett. 457*, 323−326.
52. Jencks, W. P. (1969) *Catalysis in Chemistry and Enzymology*, McGraw-Hill, New York.
53. Fehrst, A. (1985) *Enzyme Structure and Mechanism*, 2nd ed., W. H. Freeman and Co., New York.
54. Creighton, T. C. (1993) in *Proteins. Structures and Molecular Properties*, 2nd ed., W. H. Freeman and Co., New York.
55. Stock, A., M., Koshland, D. E., Jr., and Stock, J. B. (1985) *Proc. Natl. Acad. Sci. U.S.A. 82*, 7989−7993.
56. Stock, J. B., Surette, M. G., Levit, M., and Park, P. (1995) in *Two-Component Systems* (Hoch, J., and Silhavy, T., Eds.) pp 25−52, ASM Press, Washington, DC.

BI001100K